European Radiology
https://doi.org/10.1007/s00330-019-06276-8

MAGNETIC RESONANCE

Hepatic fat is superior to BMI, visceral and pancreatic fat as a potential risk biomarker for neurodegenerative disease

Ebba Beller[1,2] · Roberto Lorbeer[2] · Daniel Keeser[2] · Franziska Schoeppe[2] · Sabine Sellner[2] · Holger Hetterich[2] · Fabian Bamberg[3,4] · Christopher L. Schlett[3,4] · Annette Peters[5] · Birgit Ertl-Wagner[2,6] · Sophia Stoecklein[2]

Received: 31 January 2019 / Revised: 6 May 2019 / Accepted: 16 May 2019

Abstract

Objectives Prior studies relating body mass index (BMI) to brain volumes suggest an overall inverse association. However, BMI might not be an ideal marker, as it disregards different fat compartments, which carry different metabolic risks. Therefore, we analyzed MR-based fat depots and their association with gray matter (GM) volumes of brain structures, which show volumetric changes in neurodegenerative diseases.

Methods Warp-based automated brain segmentation of 3D FLAIR sequences was obtained in a population-based study cohort. Associations of temporal lobe, cingulate gyrus, and hippocampus GM volume with BMI and MR-based quantification of visceral adipose tissue (VAT), as well as hepatic and pancreatic proton density fat fraction ($PDFF_{hepatic}$ and $PDFF_{panc}$, respectively), were assessed by linear regression.

Results In a sample of 152 women (age 56.2 ± 9.0 years) and 199 men (age 56.1 ± 9.1 years), we observed a significant inverse association of $PDFF_{hepatic}$ and cingulate gyrus volume ($p < 0.05$) as well as of $PDFF_{hepatic}$ and hippocampus volume ($p < 0.05$), when adjusting for age and sex. This inverse association was further enhanced for cingulate gyrus volume after additionally adjusting for hypertension, smoking, BMI, LDL, and total cholesterol ($p < 0.01$) and also alcohol ($p < 0.01$). No significant association was observed between $PDFF_{hepatic}$ and temporal lobe and between temporal lobe, cingulate gyrus, or hippocampus volume and BMI, VAT, and $PDFF_{panc}$.

Conclusions We observed a significant inverse, independent association of cingulate gyrus and hippocampus GM volume with hepatic fat, but not with other obesity measures. Increased hepatic fat could therefore serve as a marker of high-risk fat distribution.

Key Points

- *Obesity is associated with neurodegenerative processes.*
- *In a population-based study cohort, hepatic fat was superior to BMI and visceral and pancreatic fat as a risk biomarker for decreased brain volume of cingulate gyrus and hippocampus.*
- *Increased hepatic fat could serve as a marker of high-risk fat distribution.*

Keywords Obesity · Magnetic resonance imaging · Liver steatosis · Cingulate gyrus · Hippocampus

Birgit Ertl-Wagner and Sophia Stoecklein contributed equally to this work.

✉ Ebba Beller
Ebba.Beller@med.uni-rostock.de

[1] Department of Diagnostic and Interventional Radiology, University Hospital, Ernst-Heydemann-Str. 6, 18057 Rostock, Germany

[2] Department of Radiology, Ludwig-Maximilians University Munich, Munich, Germany

[3] Department of Diagnostic and Interventional Radiology, Medical Center-University of Freiburg, Faculty of Medicine, University of Freiburg, Freiburg, Germany

[4] University Heart Center Freiburg-Bad Krozingen, Bad Krozingen, Germany

[5] Helmholtz Zentrum München, German Research Center for Environmental Health, Institute of Epidemiology II, Neuherberg, Germany

[6] Department of Medical Imaging, The Hospital for Sick Children, University of Toronto, Toronto, Canada

Published online: 11 June 2019

Abbreviations

AFNI	Analyses of functional images
BMI	Body mass index
FAST	FMRIB's automated segmentation tool
FLAIR	Fluid attenuation inversion recovery
FLIR	FMRIB's linear registration tool
FMRIB	Functional magnetic resonance imaging of the brain
FNIRT	FMRIB's non-linear image registration tool
GM	Gray matter
KORA	Cooperative Health Research in the Region of Augsburg
NAFLD	Nonalcoholic fatty liver disease
PDFF	Proton density fat fraction
TBV	Total brain volume
VIBE	Volume interpolated body examination
VAT	Visceral adipose tissue

Introduction

Obesity is a growing health concern globally and has been linked to an increased risk for conditions such as cardiovascular disease, diabetes, osteoarthritis, various forms of cancer, and depression [1, 2]. Regarding cognitive domains, there is evidence that obesity might affect inhibitory and executive control and working memory [3, 4]. Prior research suggests an overall inverse association of BMI with brain volume, for example in the temporal lobe [5, 6] and the hippocampal formation [7], both of which play an important role in memory and learning [8]. Furthermore, several studies suggest an inverse association between body weight and thinning of the cingulate cortex [9, 10], a region which is known to be engaged in memory-related functions [11, 12]. Moreover, human adiposity has been associated with a higher risk of neurodegenerative processes, such as Alzheimer's disease and vascular dementia [13, 14].

The most widely used and accepted approach for the measurement and classification of excess body fatness is the body mass index (BMI) [2]. However, BMI might not be an ideal marker, as it disregards different fat compartments, which might carry a variable extent of metabolic risks. For example, increased visceral adipose tissue (VAT), rather than generalized obesity, is associated with diabetogenic, atherogenic, prothrombotic, and proinflammatory alterations and an increased cardio-metabolic risk profile [15, 16]. Similarly, nonalcoholic fatty liver disease (NAFLD) and pancreatic steatosis are associated with a high prevalence of metabolic syndrome [17, 18]. Abdominal obesity and increased hepatic fat content in NAFLD have furthermore been linked to neurodegenerative processes [19, 20].

To improve our understanding of the relationship between fat distribution and neurodegenerative processes, we analyzed MR-based local fat depots of the abdomen and their association with gray matter (GM) volumes of the temporal lobe, hippocampus, and cingulate gyrus. Defining an imaging marker of high-risk fat distribution might have important implications for prevention strategies.

Methods

Study design and population

Subjects were derived from the "Cooperative Health Research in the Region of Augsburg" (KORA) F4 cohort, a prospective case-control study in southern Germany [21]. Briefly, participants with prediabetes, diabetes, and controls, who had no contraindications to MRI, and no prior history of cardiovascular disease (no percutaneous coronary intervention, myocardial infarction, bypass graft, peripheral artery disease, or stroke) underwent whole-body MRI. The whole-body MR imaging protocol was tailored for the assessment of the cerebrovascular, cardiovascular, and metabolic system. Details of the recruitment of the study sample as well as the study protocol have been previously described [22]. The study was approved by the local institutional review board of the Ludwig-Maximilians-University Munich. Informed written consent was obtained from all participants.

Assessment of population characteristics

Metabolic risk factors of the study population were collected as part of the KORA study design and have been previously described in detail by Bamberg and colleagues [21]. BMI was defined as weight (kilograms) divided by the height squared (square meter). Diabetes was defined as fasting glucose ≥ 7.0 mmol/l (126 mg/dl) and/or 2-h serum glucose ≥ 11.1 mmol/l (200 mg/dl) according to the WHO recommendations [23]. Subjects were classified as smokers if they reported current, regular, or sporadic cigarette smoking. Hypertension was defined as systolic blood pressure of at least 140 mmHg, diastolic blood pressure of at least 90 mmHg, or current antihypertensive treatment. Alcohol consumption was classified according to the anamnesis of no alcohol consumption at all, moderate alcohol consumption (0.1–39.9 g/day for men and 0.1–19.9 g/day for women) and heavy alcohol consumption (≥ 40 g/day for men and ≥ 20 g/day for women) [24].

MR image acquisition

All data were acquired using a 3-T Magnetom Skyra (Siemens Healthineers) with a whole-body radiofrequency coil-matrix system. MRI examinations of the brain, of the cardiovascular system, and of adipose tissue compartments of the chest and

abdomen were performed. The complete imaging protocol has been previously described in detail [22]. As part of the imaging protocol, a 3D fluid attenuation inversion recovery (FLAIR) sequence of the brain was obtained, which included the following parameters: TI 1800 ms, TR 5000 ms, TE 389 ms, flip angle 120°, isotropic in-plane resolution 0.5 mm, slice thickness 0.9 mm, matrix size 256 × 256, and FOV 245 × 245 mm. For the quantification of visceral adipose tissue, a two-point Dixon gradient-echo sequence was used with the following parameters: TR 4.06 ms, TE 1.26, 2.49 ms, flip angle 9°, isotropic in-plane resolution 1.7 mm, slice thickness 1.7 mm, matrix size 256 × 256, and FOV 488 × 716 mm. Hepatic and pancreatic lipid content was quantified by employing multi-echo Dixon based on a volume interpolated body examination (VIBE) sequence using the following parameters: TR 8.90 ms, six TEs ranging from 1.23 to 7.38 ms, flip angle 4°, slice thickness 4 mm, matrix size 256 × 256; confounding effects of spectral complexity of fat and T2* decay were taken into account for the estimation of liver PDFF [25].

MR image analysis

All image analyses were conducted on dedicated off-line workstations by independent readers who were unaware of the clinical status.

Neuroanatomical volumes A warp-based automated brain segmentation was applied to the 3D FLAIR datasets of the brain. Images were pre-processed using FSL 5.0.9 (http://www.fmrib.ox.ac.uk/fsl/index.html) and AFNI (analyses of functional images) (http://afni.nimh.nih.gov/afni). Following brain extraction [26], the images were reoriented and segmented using FMRIB's Automated Segmentation Tool (FAST) [26]. Individual images were warped onto the Automatic Anatomical Labeling (AAL) atlas [27] in MNI standard space, applying linear and non-linear registration as implemented in FMRIB's linear (FLIRT) and non-linear image registration tool (FNIRT) [28]. Total GM, white matter, and cerebrospinal fluid, as well as volumetric measures of 116 atlas regions (45 cortical and subcortical regions in each hemisphere and 26 cerebellar regions [29]), were calculated. In an evaluation study, the results of FLAIR-based segmentation were compared with corresponding segmentation results based on T1-weighted images [30]. In the current study, we only used GM volumes of the temporal lobe, hippocampus, and cingulate gyrus for analysis with a Pearson correlation of > 0.8 ($p < 0.001$), when compared with results of T1-weighted segmentation (Fig. 1).

Visceral adipose tissue Based on the 3D VIBE-Dixon sequence, a fat selective tomogram was calculated (slice thickness 5 mm at 5-mm increment). Visceral adipose tissue (VAT) from the level of the femoral head to the diaphragm was semi-automatically quantified with an in-house algorithm based on Matlab R2013a [31]. All segmentations were manually adjusted if necessary.

Hepatic and pancreatic fat content Mean $PDFF_{hepatic}$ was measured by drawing a region of interest manually on one

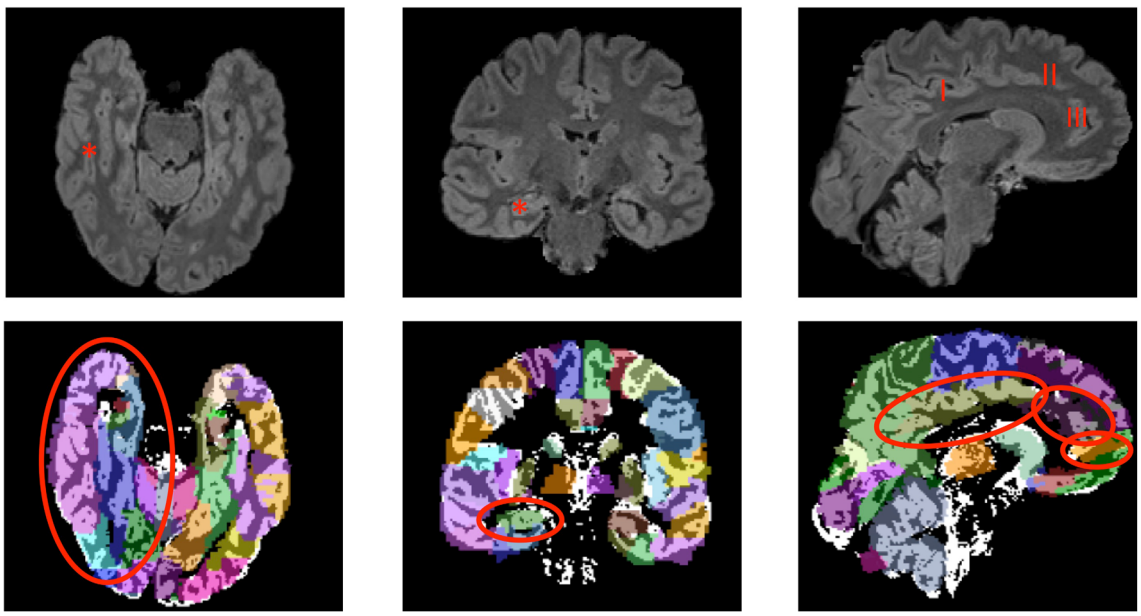

Fig. 1 Automated warp-based segmentation of 3D FLAIR datasets of the brain. A representative example of warp-based FLAIR segmentation of the right temporal lobe (asterisk), including the hippocampus, parahippocampus, amygdala, fusiform gyrus, heschl gyrus, superior, middle, and inferior temporal gyrus in axial plane (left panel), of the hippocampus (astersik) in coronal plane (middle panel) and of the cingulate gyrus (right panel), including the posterior (I), middle (II), and anterior portion (III)

slice at the level of the portal vein avoiding large vessels and surrounding extrahepatic tissue [32] (Fig. 2a). Mean $PDFF_{pancreatic}$ was assessed of the pancreatic head, body, and tail by manually drawing circular regions of interest of approximately 100 mm^2 in different MRI slices [33] (Fig. 2b).

Correcting brain volumes for total intracranial volume

Brain volumes were corrected for total intracranial volume (ICV) by using the residual method. ICV was calculated by adding up GM, WM, and CSF volumes [34]. The residual-corrected volumes were expressed as $volume_{corrected} = volume_{absolute} - b(ICV - \overline{ICV})$, where b is the slope of the linear regression of $volume_{absolute}$ over ICV across all subjects, ICV is the subject's ICV, and $\overline{ICV}$ is the mean ICV across all subjects [35, 36].

Statistical analysis

Demographics, clinical characteristics, and brain volumes were stratified by sex and summarized by mean and standard deviation for continuous variables or number and percentage for categorical variables. The differences between women and men were assessed by t test or chi-square test, respectively.

Associations of obesity markers including BMI, MR-based estimates of visceral, hepatic, and pancreatic adipose tissue with ICV-corrected brain volumes of temporal lobe, hippocampus, and cingulate gyrus were assessed using linear regression models providing β-coefficients with 95% confidence intervals for standard deviation increase of obesity markers. Models were adjusted stepwise for age, sex (model A), hypertension, and smoking status (model A+B). The regression model testing the impact of MR-based estimates of visceral, hepatic, and pancreatic adipose tissue an brain volumes was additionally adjusted for BMI, LDL, total cholesterol (model C), and alcohol consumption (model D). A p value of < 0.05 was considered statistically significant. Assumption of linearity and normal distributions of residuals were checked visually.

Statistical analyses were performed using Stata 14.1 (Stata Corporation).

Results

Population characteristics

Among 400 enrolled subjects of the FF4 cohort who underwent whole-body MRI, a total of 351 subjects were included in the present analysis with complete image acquisition and sufficient image quality. Demographic and risk profiles of the study participants stratified by sex (56.7% males) are provided in Table 1. No significant difference in BMI was observed between men and women ($p = 0.13$). However, men had a significantly greater amount of visceral adipose tissue, hepatic fat fraction, and pancreatic fat fraction compared with women ($p < 0.001$), whereas women had a significantly larger amount of subcutaneous adipose tissue and a significantly smaller waist-to-hip ratio compared with men ($p < 0.001$). Moreover, men smoked significantly more cigarettes (measured in pack-years), had significantly higher triglyceride levels and lower HDL levels, and had significantly longer time of education compared with women ($p < 0.001$).

Gender differences in GM brain volume of the hippocampus and cingulate gyrus

Table 2 displays ICV-corrected GM brain volumes of temporal lobe, hippocampus, and cingulate gyrus of the study participants stratified by sex. There was no significant difference between men and women in GM brain volume of the temporal lobe. However, ICV-corrected GM volumes of cingulate gyrus and hippocampus were significantly larger in women compared with men (< 0.001).

Associations between adiposity markers and GM brain volumes

In multivariable linear regression analyses, a higher amount of hepatic fat content was associated with smaller ICV-corrected

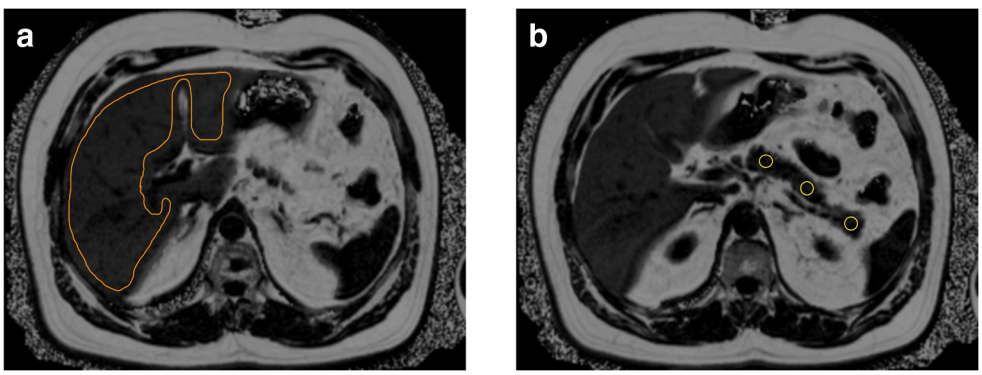

Fig. 2 MRI-based assessment of hepatic and pancreatic fat content. A representative example of $PDFF_{hepatic}$ (**a**) and $PDFF_{pancreatic}$ (**b**) measurements using a multi-echo Dixon sequence

Table 1 Characteristics of the study population, stratified by sex

Total $n = 351$	Women $n = 152$	Men $n = 199$	p value*
Age (years)	56.2 (± 9.0)	56.1 (± 9.1)	0.853
Weight (kg)	73.3 (± 15.0)	89.6 (± 13.8)	< 0.001
Height (cm)	163.4 (± 6.6)	178.0 (± 6.7)	< 0.001
BMI (kg/m^2)	27.5 (± 5.6)	28.3 (± 4.2)	0.125
BMI category (%):			0.002
< 18.5 kg/m^2	1 (0.7%)	0 (0%)	
18.5–24.9 kg/m^2	56 (36.8%)	39 (19.6%)	
25.0–29.9 kg/m^2	51 (33.6%)	100 (50.3%)	
30.0–34.9 kg/m^2	28 (18.4%)	46 (23.1%)	
35.0–39.9 kg/m^2	10 (6.6%)	10 (5.0%)	
40+ kg/m^2	6 (4.0%)	4 (2.0%)	
Waist circumference (cm)	91.3 (± 13.9)	103.1 (± 11.9)	< 0.001
Hip circumference (cm)	106.8 (± 10.9)	106.7 (± 7.5)	0.899
Waist to hip ratio	0.85 (± 0.07)	0.96 (± 0.07)	< 0.001
Waist/height ratio	0.56 (± 0.09)	0.58 (± 0.07)	0.020
Total adipose tissue (l/m^2)	4.45 (± 2.26)	4.11 (± 1.67)	0.112
Visceral adipose tissue (l/m^2)	1.08 (± 0.73)	1.80 (± 0.84)	< 0.001
Subcutaneous adipose tissue (l/m^2)	3.38 (± 1.66)	2.33 (± 1.00)	< 0.001
Hepatic fat fraction (%)	5.87 (± 7.49)	9.78 (± 8.4)	< 0.001
Pancreatic fat fraction (%)	6.07 (± 5.15)	8.66 (± 7.81)	< 0.001
Total cholesterol (mg/dl)	220.9 (± 35.4)	215.7 (± 37.9)	0.191
HDL (mg/dl)	70.9 (± 18.1)	55.2 (± 14.9)	< 0.001
LDL (mg/dl)	138.2 (± 32.6)	141.6 (± 32.8)	0.333
Triglycerides (mg/dl)	101.2 (± 45.8)	151.4 (± 97.0)	< 0.001
Diabetes mellitus	13 (8.6%)	32 (16.1%)	0.037
Smoking status			0.041
Never smoker	66 (43.4%)	63 (31.7%)	
Former smoker	53 (34.9%)	94 (47.2%)	
Current smoker	33 (21.7%)	42 (21.1%)	
Pack-years	8.2 (± 12.5)	16.7 (± 21.0)	< 0.001
Alcohol consumption			< 0.001
Alcohol consumption (g/day)	8.0 (± 11.8)	24.8 (± 24.6)	
No alcohol consumption	54 (35.5%)	35 (17.6%)	
Moderate alcohol consumption (men, 0.1–39.9; women, 0.1–19.9 g/day)	73 (48.0%)	111 (55.8%)	
Heavy alcohol consumption (men, ≥ 40; women, ≥ 20 g/day)	25 (16.5%)	53 (26.6%)	
Hypertension	42 (27.6%)	75 (37.7%)	0.048
Systolic BP (mmHg)	113 (± 15)	126 (± 16)	< 0.001
Diastolic BP (mmHg)	72 (± 9)	78 (± 11)	< 0.001
Education time (years)	11.6 (± 2.3)	12.7 (± 2.7)	< 0.001
Physical activity in categories			0.051
1 = regularly > 2 h a week	41 (27%)	62 (31.2%)	
2 = regularly approx. 1 h a week	59 (38.8%)	56 (28.1%)	
3 = irregularly approx. 1 h a week	25 (16.5%)	26 (13.1%)	
4 = almost none or no exercise	27 (17.8%)	55 (27.6%)	

Values in mean ± standard deviation or number and percentage, *p values are from t test or chi-square test

Table 2 Brain volumes, stratified by sex

Neuroanatomical structure	Women	Men	*p* value
Temporal lobe GM (ml)	79.9 (± 4.4)	78.7 (± 5.5)	0.025
Hippocampus (ml)	8.3 (± 0.5)	8.0 (± 0.6)	< 0.001
Cingulate gyri (ml)	28.0 (± 1.9)	27.2 (± 2.1)	< 0.001

All neuroanatomical volumes are ICV-corrected by using the residual method

GM volume of the cingulate gyrus ($\beta = -0.21$ [95%CI −0.42,− 0.01], $p < 0.05$) and hippocampus ($\beta = -0.07$ [95%CI − 0.13, − 0.01], $p < 0.05$) when adjusting for age and sex. In contrast, there was no significant association between ICV-corrected GM volume of cingulate gyrus or hippocampus and BMI, visceral, or pancreatic fat content. Additional adjustment for hypertension, smoking, BMI, LDL, and total cholesterol further enhanced the inverse association between $PDFF_{hepatic}$ and GM volume of the cingulate gyrus ($\beta = -0.33$ [95%CI − 0.57, 0.09], $p < 0.01$). However, $PDFF_{hepatic}$ was no longer statistically associated with hippocampal volume ($\beta = -0.06$ [95%CI − 0.14, 0.01]). After additional adjustment for alcohol, the inverse association between $PDFF_{hepatic}$ and GM volume of the cingulate gyrus remained significant ($\beta = -0.34$ [95%CI − 0.58, − 0.1], $p < 0.01$). There was no statistical association between all adiposity markers and ICV-corrected GM temporal lobe volume in all three models (Table 3).

Discussion

This cohort study data indicate an inverse association of GM volume of cingulate gyrus and hippocampus with increased $PDFF_{hepatic}$. After controlling for smoking and hypertension, BMI, LDL, total cholesterol, and alcohol, $PDFF_{hepatic}$ remained inversely associated with GM cingulate gyrus volume. These findings suggest that the inverse relationship between liver fat and GM volume of the cingulate gyrus cannot be sufficiently explained by cardiovascular risk factors, global fat markers, or alcohol consumption alone.

Several studies found an association between increased global BMI and reduction in regional GM brain volume, although the location and magnitude of these reductions have been inconsistent [10, 37, 38]. This could be explained by the fact that BMI does not directly represent organ-based pathological states, such as hepatic or pancreatic steatosis, nor does it account for different fat compartments, which carry different metabolic risks [39]. BMI may also not be helpful in individuals with high muscle mass (e.g., body builders), in certain ethnic backgrounds [40] or in elderly individuals with decreasing muscle mass and increasing adipose tissue [41]. Therefore, local fat depots instead of global adiposity may play a more important role in various metabolic and vascular pathologic conditions, resulting in accelerated brain aging. For example, NAFLD is associated with an increased risk of clinical and subclinical cardiovascular diseases [42–44], which in turn contribute directly to changes in brain structure and function [45]. Additional shared risk factors between liver steatosis and brain aging include physical inactivity [46], inflammation [47], hormonal alterations such as insulin resistance [48], endothelial dysfunction [49], and change in levels of secreted hepatokines [50]. Although the abundance of literature indicates an association, only a few studies have investigated the direct link between hepatic steatosis and markers of brain aging, to our knowledge: In a recent study from the cohort of the Framingham Offspring study, NAFLD, assessed by CT, was significantly associated with a smaller total brain volume (TBV) [51]. In a prior study in overweight subjects, increased CT-assessed, hepatic fat was associated with reduced brain tissue integrity in both GM and WM

Table 3 Association of obesity markers with brain volumes

	Model	Cingulate gyri	Hippocampus	Temporal lobe
Per 1 SD increment		β (95%CI)	β (95%CI)	β (95%CI)
BMI total	A	0.05 (− 0.15, 0.25)	− 0.03 (− 0.09, 0.03)	0.05 (− 0.38, 0.48)
Visceral adipose tissue	A	− 0.02 (− 0.26, 0.21)	− 0.03 (− 0.1, 0.04)	0.03 (− 0.46, 0.53)
	B	− 0.17 (− 0.53, 0.19)	0.01 (− 0.1, 0.11)	0.1 (− 0.66, 0.86)
	C	− 0.18 (− 0.54, 0.18)	0 (− 0.11, 0.11)	0.05 (−0.71, 0.81)
Hepatic adipose tissue	A	− 0.21 (− 0.42, − 0.01)*	− 0.07 (− 0.13, − 0.01)*	− 0.25 (− 0.7, 0.2)
	B	− 0.33 (− 0.57, − 0.09)**	− 0.06 (− 0.14, 0.01)	− 0.27 (−0.79, 0.25)
	C	− 0.34 (− 0.58, − 0.1)**	− 0.07 (− 0.14, 0)	− 0.31 (− 0.82, 0.21)
Pancreatic adipose tissue	A	− 0.14 (− 0.35, 0.07)	− 0.04 (− 0.1, 0.03)	− 0.26 (− 0.71, 0.19)
	B	− 0.16 (− 0.38, 0.06)	− 0.03 (− 0.1, 0.04)	− 0.23 (− 0.71, 0.24)
	C	− 0.16 (− 0.38, 0.06)	− 0.03 (− 0.09, 0.04)	− 0.22 (− 0.69, 0.25)

β-coefficients are from linear regression models adjusted for age and sex (model A), additionally adjusted for hypertension, smoking, BMI, LDL, and total cholesterol (model B) and also alcohol (model C), *$p < 0.05$; **$p < 0.01$; *SD*, standard deviation

[52]. Both study results were independent of VAT and cardiovascular risk factors. A study by VanWagner and colleagues showed that NAFLD, quantified by CT, was also associated with decreased TBV, even after controlling for BMI, but not independent of VAT [19]. Our study confirms the inverse association of increasing hepatic fat and GM brain volume, which we found to be statistically significant for the cingulate gyrus. This association was independent of cardiovascular risk factors, global fat markers, and alcohol consumption.

In our study, men had significantly greater amounts of visceral, hepatic, and pancreatic fat contents while women had a significantly larger amount of subcutaneous adipose tissue and a significantly smaller waist-to-hip ratio. These differences in regional fat storage represent, to some extent, gender-related differences in fat distribution [53, 54]. Interestingly, there was also a significant difference in brain volume, when comparing men and women. Men had significantly smaller GM volumes of cingulate gyrus and hippocampus, when compared with women. Since reduced cingulate gyrus and hippocampus GM volume were both associated with increased $PDFF_{hepatic}$, these differences in brain volume may therefore be related to the gender-specific fat distribution.

To our knowledge, this is the first study to compare GM brain volumes with quantitative MRI measures of local fat depots, including visceral, hepatic, and pancreatic fat. All proposed MRI fat markers are non-invasively available without radiation exposure and can easily be obtained within abdominal MR imaging. Especially radiologists, cardiologists, and medical specialists in the field of preventive medicine should be aware of the potential gain of information about cardiometabolic health by using all available information on a specific examination [55]. This information can improve the early detection of potentially high-risk fat distribution patterns and the personalized risk workup in a given patient [55, 56]. Moreover MRI-PDFF, which was used in our study to quantify liver fat, has proven to be an accurate, reproducible biomarker of hepatic steatosis [57, 58]. Another strength of this study is the population-based setting with metabolic and demographic characterization of the sample.

There are also several limitations to this study. In previous studies, automated brain volumetry has been mainly based on T1-weighted MR images [59]. Since participants of the KORA study did not obtain 3D T1-weighted images of the brain, 3D FLAIR images were used for automated warp-based brain segmentation. However, this method was evaluated by comparing FLAIR- with T1-based segmentation results in an independent sample of healthy controls, and only neuroanatomical structures with a strong correlation between both MRI sequences were used for analysis in the present study [30]. Another limitation might be potential under-reporting of alcohol consumption among drinkers.

In summary, we observed a significant inverse association of the cingulate gyrus and hippocampus GM volume and hepatic fat fraction, but no significant association with BMI, VAT, or pancreatic fat content. Increased hepatic fat may therefore have a greater impact on neurodegenerative processes compared with other fat depots and could serve as a marker of high-risk fat distribution. These findings may improve our understanding of the mechanisms underlying the relationship of high-risk fat distribution and neurodegenerative processes with potentially important implications for prevention strategies.

Funding This research was funded in-part by the German Research Foundation (DFG, Bonn, Germany; grant-number 245222810). The KORA study was initiated and financed by the Helmholtz Zentrum München—German Research Center for Environmental Health, which is funded by the German Federal Ministry of Education and Research (BMBF) and by the State of Bavaria. The KORA-MRI sub-study was supported by an unrestricted research grant from Siemens Healthcare.

Compliance with ethical standards

Guarantor The scientific guarantor of this publication is Sophia Stoecklein.

Conflict of interest The authors of this manuscript declare no relationships with any companies whose products or services may be related to the subject matter of the article.

Statistics and biometry No complex statistical methods were necessary for this paper.

Informed consent Written informed consent was obtained from all subjects (patients) in this study.

Ethical approval Institutional Review Board approval was obtained.

Methodology
- Retrospective
- Diagnostic or prognostic study
- Performed at one institution

References

1. Prickett C, Brennan L, Stolwyk R (2015) Examining the relationship between obesity and cognitive function: a systematic literature review. Obes Res Clin Pract 9:93–113
2. Cornier MA, Marshall JA, Hill JO, Maahs DM, Eckel RH (2011) Prevention of overweight/obesity as a strategy to optimize cardiovascular health. Circulation 124:840–850
3. Elias MF, Elias PK, Sullivan LM, Wolf PA, D'Agostino RB (2003) Lower cognitive function in the presence of obesity and hypertension: the Framingham heart study. Int J Obes Relat Metab Disord 27:260–268
4. Gunstad J, Paul RH, Cohen RA, Tate DF, Gordon E (2006) Obesity is associated with memory deficits in young and middle-aged adults. Eat Weight Disord 11:e15–e19
5. Gustafson D, Lissner L, Bengtsson C, Bjorkelund C, Skoog I (2004) A 24-year follow-up of body mass index and cerebral atrophy. Neurology 63:1876–1881

6. Bobb JF, Schwartz BS, Davatzikos C, Caffo B (2014) Cross-sectional and longitudinal association of body mass index and brain volume. Hum Brain Mapp 35:75–88
7. Dhikav V, Anand K (2011) Potential predictors of hippocampal atrophy in Alzheimer's disease. Drugs Aging 28:1–11
8. Squire LR, Zola-Morgan S (1991) The medial temporal lobe memory system. Science 253:1380–1386
9. Driscoll I, Beydoun MA, An Y et al (2012) Midlife obesity and trajectories of brain volume changes in older adults. Hum Brain Mapp 33:2204–2210
10. Raji CA, Ho AJ, Parikshak NN et al (2010) Brain structure and obesity. Hum Brain Mapp 31:353–364
11. Weible AP (2013) Remembering to attend: the anterior cingulate cortex and remote memory. Behav Brain Res 245:63–75
12. Hampson M, Driesen NR, Skudlarski P, Gore JC, Constable RT (2006) Brain connectivity related to working memory performance. J Neurosci 26:13338–13343
13. Emmerzaal TL, Kiliaan AJ, Gustafson DR (2015) 2003–2013: a decade of body mass index, Alzheimer's disease, and dementia. J Alzheimers Dis 43:739–755
14. Pedditizi E, Peters R, Beckett N (2016) The risk of overweight/obesity in mid-life and late life for the development of dementia: a systematic review and meta-analysis of longitudinal studies. Age Ageing 45:14–21
15. Franzosi MG (2006) Should we continue to use BMI as a cardiovascular risk factor? Lancet 368:624–625
16. Despres JP (2006) Is visceral obesity the cause of the metabolic syndrome. Ann Med 38:52–63
17. Smits MM, van Geenen EJ (2011) The clinical significance of pancreatic steatosis. Nat Rev Gastroenterol Hepatol 8:169–177
18. Yang KC, Hung HF, Lu CW, Chang HH, Lee LT, Huang KC (2016) Association of non-alcoholic fatty liver disease with metabolic syndrome independently of central obesity and insulin resistance. Sci Rep 6:27034
19. VanWagner LB, Terry JG, Chow LS et al (2017) Nonalcoholic fatty liver disease and measures of early brain health in middle-aged adults: the CARDIA study. Obesity (Silver Spring) 25:642–651
20. Whitmer RA, Gustafson DR, Barrett-Connor E, Haan MN, Gunderson EP, Yaffe K (2008) Central obesity and increased risk of dementia more than three decades later. Neurology 71:1057–1064
21. Holle R, Happich M, Lowel H, WichmannHE (2005) KORA–a research platform for population based health research. Gesundheitswesen 67(Suppl 1):S19–S25
22. Bamberg F, Hetterich H, Rospleszcz S et al (2017) Subclinical disease burden as assessed by whole-body MRI in subjects with prediabetes, subjects with diabetes, and normal control subjects from the general population: the KORA-MRI study. Diabetes 66:158–169
23. World Health Organization (2006) Definition and diagnosis of diabetes mellitus and intermediate hyperglycemia. World Health Organization, Geneva
24. Ruf E, Baumert J, Meisinger C, Doring A, Ladwig KH (2014) Are psychosocial stressors associated with the relationship of alcohol consumption and all-cause mortality? BMC Public Health 14:312
25. Hetterich H, Bayerl C, Peters A et al (2016) Feasibility of a three-step magnetic resonance imaging approach for the assessment of hepatic steatosis in an asymptomatic study population. Eur Radiol 26:1895–1904
26. Smith SM (2002) Fast robust automated brain extraction. Hum Brain Mapp 17:143–155
27. Tzourio-Mazoyer N, Landeau B, Papathanassiou D et al (2002) Automated anatomical labeling of activations in SPM using a macroscopic anatomical parcellation of the MNI MRI single-subject brain. Neuroimage 15:273–289
28. Jenkinson M, Bannister P, Brady M, Smith S (2002) Improved optimization for the robust and accurate linear registration and motion correction of brain images. Neuroimage 17:825–841
29. Zhang C, Cahill ND, Arbabshirani MR, White T, Baum SA, Michael AM (2016) Sex and age effects of functional connectivity in early adulthood. Brain Connect 6:700–713
30. Beller E, Keeser D, Wehn A et al (2018) T1-MPRAGE and T2-FLAIR segmentation of cortical and subcortical brain regions-an MRI evaluation study. Neuroradiology. https://doi.org/10.1007/s00234-018-2121-2
31. Wurslin C, Machann J, Rempp H, Claussen C, Yang B, Schick F (2010) Topography mapping of whole body adipose tissue using a fully automated and standardized procedure. J Magn Reson Imaging 31:430–439
32. Lorbeer R, Bayerl C, Auweter S et al (2017) Association between MRI-derived hepatic fat fraction and blood pressure in participants without history of cardiovascular disease. J Hypertens 35:737–744
33. Heber SD, Hetterich H, Lorbeer R et al (2017) Pancreatic fat content by magnetic resonance imaging in subjects with prediabetes, diabetes, and controls from a general population without cardiovascular disease. PLoS One 12:e0177154
34. Dell'Oglio E, Ceccarelli A, Glanz BI et al (2015) Quantification of global cerebral atrophy in multiple sclerosis from 3T MRI using SPM: the role of misclassification errors. J Neuroimaging 25:191–199
35. Hansen TI, Brezova V, Eikenes L, Haberg A, Vangberg TR (2015) How does the accuracy of intracranial volume measurements affect normalized brain volumes? Sample size estimates based on 966 subjects from the HUNT MRI cohort. AJNR Am J Neuroradiol 36:1450–1456
36. Pintzka CW, Hansen TI, Evensmoen HR, Haberg AK (2015) Marked effects of intracranial volume correction methods on sex differences in neuroanatomical structures: a HUNT MRI study. Front Neurosci 9:238
37. Gunstad J, Paul RH, Cohen RA et al (2008) Relationship between body mass index and brain volume in healthy adults. Int J Neurosci 118:1582–1593
38. Pannacciulli N, Del Parigi A, Chen K, Le DS, Reiman EM, Tataranni PA (2006) Brain abnormalities in human obesity: a voxel-based morphometric study. Neuroimage 31:1419–1425
39. Fox CS, Massaro JM, Hoffmann U et al (2007) Abdominal visceral and subcutaneous adipose tissue compartments: association with metabolic risk factors in the Framingham Heart Study. Circulation 116:39–48
40. Cossrow N, Falkner B (2004) Race/ethnic issues in obesity and obesity-related comorbidities. J Clin Endocrinol Metab 89:2590–2594
41. Barlett HL, Puhl SM, Hodgson JL, Buskirk ER (1991) Fat-free mass in relation to stature: ratios of fat-free mass to height in children, adults, and elderly subjects. Am J Clin Nutr 53:1112–1116
42. Francque SM, van der Graaff D, Kwanten WJ (2016) Non-alcoholic fatty liver disease and cardiovascular risk: pathophysiological mechanisms and implications. J Hepatol 65:425–443
43. Wu S, Wu F, Ding Y, Hou J, Bi J, Zhang Z (2016) Association of non-alcoholic fatty liver disease with major adverse cardiovascular events: a systematic review and meta-analysis. Sci Rep 6:33386
44. Long MT, Wang N, Larson MG et al (2015) Nonalcoholic fatty liver disease and vascular function: cross-sectional analysis in the Framingham heart study. Arterioscler Thromb Vasc Biol 35:1284–1291
45. Gorelick PB, Scuteri A, Black SE et al (2011) Vascular contributions to cognitive impairment and dementia: a statement for healthcare professionals from the American heart association/American stroke association. Stroke 42:2672–2713

46. Debette S, Seshadri S, Beiser A et al (2011) Midlife vascular risk factor exposure accelerates structural brain aging and cognitive decline. Neurology 77:461–468
47. Taipale T, Seppala I, Raitoharju E et al (2018) Fatty liver is associated with blood pathways of inflammatory response, immune system activation and prothrombotic state in Young Finns Study. Sci Rep 8:10358
48. Ghareeb DA, Hafez HS, Hussien HM, Kabapy NF (2011) Non-alcoholic fatty liver induces insulin resistance and metabolic disorders with development of brain damage and dysfunction. Metab Brain Dis 26:253–267
49. Sapmaz F, Uzman M, Basyigit S et al (2016) Steatosis grade is the Most important risk factor for development of endothelial dysfunction in NAFLD. Medicine (Baltimore) 95:e3280
50. Stefan N, Haring HU (2013) The role of hepatokines in metabolism. Nat Rev Endocrinol 9:144–152
51. Weinstein G, Zelber-Sagi S, Preis SR et al (2018) Association of nonalcoholic fatty liver disease with lower brain volume in healthy middle-aged adults in the Framingham Study. JAMA Neurol 75: 97–104
52. Sala M, van der Grond J, de Mutsert R et al (2016) Liver fat assessed with CT relates to MRI markers of incipient brain injury in middle-aged to elderly overweight persons. AJR Am J Roentgenol 206:1087–1092
53. Blaak E (2001) Gender differences in fat metabolism. Curr Opin Clin Nutr Metab Care 4:499–502
54. Karastergiou K, Smith SR, Greenberg AS, Fried SK (2012) Sex differences in human adipose tissues - the biology of pear shape. Biol Sex Differ 3:13
55. Bos D, Leening MJG (2018) Leveraging the coronary calcium scan beyond the coronary calcium score. Eur Radiol 28:3082–3087
56. Graffy PM, Pickhardt PJ (2016) Quantification of hepatic and visceral fat by CT and MR imaging: relevance to the obesity epidemic, metabolic syndrome and NAFLD. Br J Radiol 89:20151024
57. Ajmera V, Park CC, Caussy C et al (2018) Magnetic resonance imaging proton density fat fraction associates with progression of fibrosis in patients with nonalcoholic fatty liver disease. Gastroenterology 155:307–310 e302
58. Idilman IS, Aniktar H, Idilman R et al (2013) Hepatic steatosis: quantification by proton density fat fraction with MR imaging versus liver biopsy. Radiology 267:767–775
59. Lindig T, Kotikalapudi R, Schweikardt D et al (2017) Evaluation of multimodal segmentation based on 3D T1-, T2- and FLAIR-weighted images - the difficulty of choosing. Neuroimage. https://doi.org/10.1016/j.neuroimage.2017.02.016